EuroSun2026

BUILDING THERMAL SELF-SUFFICIENCY FUNCTIONS OF PV DRIVEN HEAT PUMPS CHARGING THERMAL ENERGY AND BATTERY STORAGES

Lukas Omlin, Paul Gantenbein, Xavier Daguenet
SPF Institute for Solar Technology, OST Eastern Switzerland University of Applied Sciences
e-mail address - lukas.omlin@ost.ch

Abstract

A PV electric driven compressor heat pump system for space heating and domestic hot water with different large size thermal energy storage (near surface thermal energy storage, phase change material thermal energy storage, ice thermal energy storage and water thermal energy storage) for single family house applications were defined. Simulation templates were set up, simulations were performed, and the results show a remarkable increase of the thermal self-sufficiency in function of the large storage up to a size of about 15 m^3, for the storage materials water and ice. After this storage volume a smooth increase is observed for all types of storage. The initial value of 70 % - without a large storage - can be explained by the system concept of two small thermal storages, one for domestic hot water and one for space heating and covering the short-term demand therein. The self-sufficiency data in function of the storage size were fitted with an exponential function. Even at all types of large storages the thermal self-sufficiency does not reach 100 % except a battery is implemented in the system i.e. at certain demand, the heat pump can run by el. energy supplied by the battery. The results show a similar functional behavior of the solar energy share with a water storage in a single-family house where, in parallel configuration, solar thermal collectors and heat pump systems cover the space heating and domestic hot water demand.

Keywords: Solar Space Heating & Domestic Hot Water, PV Electric Driven Compressor, Solar Thermal, Storage Volume, Thermal Self-Sufficiency

1. Introduction

The energy transition in the building sector for decarbonization, and thus omitting fossil fuels, with the application of renewable sources is a challenge. Renewable energy sources are subject to seasonal or diurnal (solar) fluctuations. And thus, to support daytime and seasonal independence, energy storage can take and fulfil these tasks. Research on long-term thermal energy storage has high priority worldwide for heating, domestic hot water and for cooling as well.

Due to technology transition from thermal (predominantly) to electric driven (even for space heating and hot water demand) heating systems and the simplicity[1] of application, PV electricity has a dominant role in the application of solar irradiation as an energy source compared to solar thermal. In this context our study concentrates on the (attribute) of thermal-self-sufficiency of a building, i.e. a single-family house (SFH), where the space heating (space heating SH with warm water thorough floor heating) and domestic hot water (DHW) is prepared – as far as possible - by solar PV electricity driven heat pumps. In case of shortage of PV energy but energy demand in the building, the electric energy stems from the public electricity grid.

With the sun as the (main) energy source and the building as the energy sink (space heating SH and domestic hot water DHW) a probable source (energy available) -sink (energy demand) relation - independent of the “energy transfer carrier” (electric in a cable; thermal in a fluid) is the task. Based on these general considerations simulations templates for a single-family house (SFH) - with PV driven-building energy systems - were defined. And a thermal energy storage in a building is considered, where no soil prob (borehole) is allowed due to ground water (pollution) or any other reason, for example, where the building is or will be under tunneled. As main system parameters (focus) served the type (water etc.) and size (volume, volumetric energy density) of the long-term thermal energy storage. And as types of storages near surface thermal energy storage (NTES), phase change

[1] We do not claim electric systems are simple – but, for example, the installation of the power lines of a PV panel field is – we guess - simpler than the piping for the heat transfer fluid of a solar thermal collector field.

material thermal energy storage (PCM), ice thermal energy storage (ICE) and water thermal energy storage (WTES) were used. At this level of investigation, relevant economic issues were considered by market available components (PV panels, batteries, heat pumps, storage tanks pumps etc.) but, due to local and time relevant reasons, prices (for example Euros or CHF etc.) were not considered.

In the following we present the performed parameter study. There, the size of the thermal energy storage – the Volume V_{STES} in m^3 - has (the dominant) priority. While the PV-panel area (A_{PV} in m^2), the battery capacity (C_{Bat} in kWh) and the power of the heat pump (P_{HP} in kW) in the first steps were kept constant. Part of the restriction in the PV-panel area is due to the limited roof area on (for example) a single-family house (SFH). The results of the work (solar PV driven systems) are compared to (the well-known) literature values of heat pump and solar thermal driven heat energy supplying systems. The restriction in these (solar thermal) systems is the use of grid electricity to run the heat pump in a parallel energy source configuration to the solar thermal collectors [C. Dennis Barley and C. Byron Winn 1978; J. V. Anderson, J. W. Michell and W. A. Beckman 1980; Duffie Beckman 2013].

2. Building energy system concept and boundary conditions

A simple building energy system was selected to supply energy for space heating (SH) and domestic hot water (DHW) preparation in buildings – single family house (SFH) applications. The energy demand profiles were selected and the renewable energy sources used are: the ambient air (air source heat pump), solar PV panels (design variable A – m^2) and the public electric grid. The location – with the relevant weather conditions - of the building is Bern in Switzerland. And, to keep the energy supplying system simple, no solar thermal nor PVT collectors were applied. Figure 1 shows an iconographic system configuration with a phase-change material (PCM) storage as a (long-term) Seasonal Thermal Energy Storage (STES) example system implementation. On the right of this figure 1, different types of STES are shown and were selected in the simulation for energy supply to the SFH.

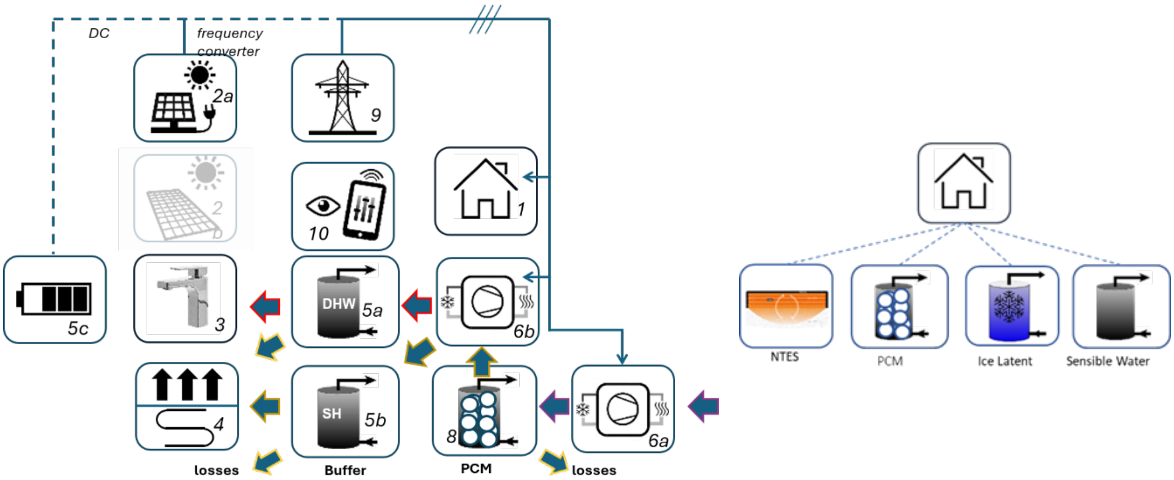

Fig. 1 (left) STES system configuration for space heating & cooling (4) and domestic hot water (3). The example shows the system for a single-family house (1) with a phase change storage PCM (8). Electric energy is supplied by PV panels (2a) and the public electric grid (9). Domestic hot water (DHW, 5a) is stored in a hot water tank, and the space heating fluid (water) is stored in a buffer tank (SH, 5b). Batteries (5c) are used for an increase of the electric and thermal self-sufficiency. Solar thermal collectors (2b) are not considered at this level of investigation. To prepare room heating and hot water a cascade of an air and water source heat pump (6a & 6b) is used. The energy supply system operates by a programmable controller (10). (right) Different STES types for SFH application – but for all the same system integration (NTES = Near Surface Thermal Energy Storage).

To determine the self-sufficiency of a single-family house (SFH) a set of four templates [Berger et al. 2022] were used, modified and extended in the Polysun® simulation software. In table 1 the boundary conditions for the building energy demand and the design variables of the PV driven energy supplying system are summarized. In this study the main design variable is volume V (m^3) of the STES, at constant PV panel area A_{PV} (m^2). To reach a high PV-energy self-consumption the programmable controller is predominantly unlocked during daytime and starts the air source heat pump 6a if a threshold PV power value is reached. The simulations were performed with the parameters listed in table 1. Due to the complexity of a reactor for the thermochemical storage (TCS) system, no simulation model is set up at this level of investigation. Therefore, a good guess is made for the TCS case based on the absorption potential energy storage density data, but the findings are not presented here.

Table 1 List of system parameters in the simulations for SFH application.

Parameter / Variable	Range	Unit	Remark
SFH Heating Energy demand Q_{demand}	45	kWh m^{-2} a^{-1}	Location Bern (solar irradiation, Tamb etc., Meteotest AG), 2 floors
Space heating cooling area A_{SH}	140	m^2	SFH, Swiss Federal Statistical Office
Room temperature T_{room}; T_{SH} inlet SH 35 °C	21 .. 23	°C	ΔT +1 (K) ~7 % more energy for SH
Buffer tank volume (SH) V_{Buffer}	600	l	SFH floor heating (T_{SH} 35 °C)
DHW consumption, 4 persons	50	liter $person^{-1}$ day^{-1}	Domestic hot water (DHW) Euro profile with morning/evening peaks
DHW temperature T_{DHW}	50	°C	hygienic aspects, shot time 60 °C
DHW tank volume V_{DHW}	300	Liter	short term storage (DHW profile)
Air source / brine heat pump HP	10 .. 15	kW	"cheapest" installation
Electricity consumption $Q_{el.}$	4500	kWh a^{-1}	daily profile in 15 Min resolution
PV Cell Type mono crystalline	180	W_p m^{-2}	Silicon (Si), south, tilt angle 35°
PV panel area[1] A_{PV}; (20) 40 (120) number of modules	65.2	m^2	design variable A_{PV}, area available on the SFH roof 11.7 kW_p; A_{PV}/A_{SH} =0.47
Battery / Capacity	25.0	kWh	some models (C_{Bat}/A_{PV}, kWh m^{-2})
Public electric grid connection (voltage U, current I, power P)	400, 40, 27.7	V, A, kW	SFH el. connection to the grid

Due to parameter ranges (some) - the simulation results are presented in the diagrams with uncertainty bars on both - abscissa and ordinate - axes.

3. System layout and building thermal self-sufficiency

The space heating (SH) and domestic hot water (DHW) system comprises a heat pump cascade with two heat pumps in series and, in regard of temperature, a STES in between. A DHW tank (300 l) and an SH buffer tank (600 l) are considered to cover peak demand and thus for a lower heat pump (HP 2; 6b) power and short-term storage. To further increase the PV-energy self-consumption the programmable controller is predominantly unlocked during daytime for the air source heat pump 1 (HP 1; available solar radiation) to charge the STES with PV electricity. This means, the basic control (controller PC 1 in figure 2) that increases self-sufficiency of the system is defined, where the STES can be charged by the PV driven heat pump (HP 1). In case a battery is implemented in the system the surplus of PV electricity can be stored in the battery (Battaglia et al.). For times of heat energy at high enough temperature in the STES ($T_{STES} \geq T_{SH} \cap$ water source heat pump inlet $T_{HPin, max}$) a bypass heat exchanger (HEX) is in the model, and the charging of the SH Buffer tank can be performed without running the second heat pump 2 (HP 2). Figure 2 shows the graphical user interface (GUI) of the simulation template with PCM storage as an example. As mentioned, the building energy system parameters are summarized in table 1. And the simulations were performed with the parameters listed in this table 1.

[1] In this study parameters relation of A_{PV}/A_{room} (PV to space heating & DHW) in the range of (0.23) .. 0.47 .. (1.63) is defined.

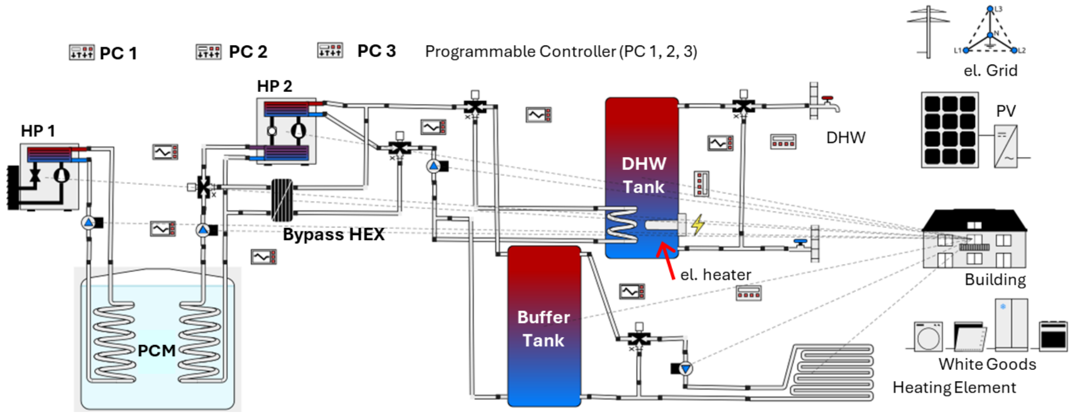

Fig. 2 Single family house system configuration with a PCM STES implemented (battery not shown). Due to predominant operation in high enough (liquid phase) temperature of the PCM storage a heat pump 2 (HP 2; 6b) bypassing heat exchanger "Bypass HEX" was added to the simulation template. PC 1, 2, 3 are programmable controllers. In this study, the electric heater (the back-up el. heater) in the DHW tank is switched off all the time.

The task to think about and to determine the thermal self-sufficiency of the building thermal energy system is crucial. And this cruciality depends on and with the dealing of electric energy. Generally, in a system which is driven by electric energy – heat pump, fluid pump, white goods etc. - one can take the electric energy is converted to heat (increasing entropy). For this reason, we account all energy used in the time-period (space heating period) of October to March of the following year – as converted to heat and contributes to space heating. This means, the white goods operation with electric energy – and a part is used for space heating.

4. Results and Discussion

In figure 3 and figure 4 the results for systems with WTES, PCM, Water ICE and near surface NTES STES in a SFH are shown. A thermal self-sufficiency of 70 % and higher is reached at a volume higher than approx. 5 m^3 to 10 m^3 for all STES types. This effect is intrinsic to the system design – a buffer tank for space heating and a domestic hot water (DHW) tank (Figure 2) – where short time thermal energy demand (covering peak demand) can be bridged.

The WTES data are shown in Figure 3, where at low volumes – below 5 m^3 - of the storage a strong increase of the thermal self-sufficiency is visible. After this size the smooth increase is more or less linear in function of the volume. And the uncertainty bars of the data account for slight differences in demand profiles, storage system implementation, sensors uncertainty and so on and forth. For comparison, literature data of the solar share (right ordinate in figure 3) in function of the water storage volume of a solar thermal building energy system are implemented in the graph. Observing the two curves shape, a coincidence of the thermal self-sufficiency and the solar share exists – but the solar share (solar thermal only) with slightly lower values. For more details, in the Appendix of this document some literature data of the graphs are reconstructed.

In all other system simulations with the storage types NTES, PCM and (water) ICE a similar thermal self-sufficiency behaviour (curve) occurs. The differences stem from the (max.) temperature level and the volumetric storage density i.e. the heat capacity $\rho(T)*c_p(T)$ and phase change or fusion enthalpy Δh_{fus} of the storage material in relation to the solid (s) to liquid (l) density change. Where in case of ICE, the storage material is the same as in the WTES, except in the ICE storage a phase change is "initiated" at 0 °C, with $\Delta h_{fus,ICE}$ = 330 kJ*kg^{-1}, and the density of ice is ρ_{ICE}(0 °C) = 916.2 kg*m^{-3} (VDI). And further, in a PCM storage, one difference to the ICE storage is the temperature level (position) of the phase transition T_{s-l} (enthalpy method applied) from solid (s) to liquid (l) and vice versa (and ice – the solid state of water - has a lower density $\rho_{ICE}(T)$ than water, but PCM has in the solid state a higher density than in the liquid state). While the PCM (salt hydrates, paraffins) have lower thermal capacities $\rho(T)*c_{p,s}(T)$ in the solid and the liquid $\rho(T)*c_{p,l}(T)$ state and the cycled temperature difference (ΔT) determines the total enthalpy difference. These thermo-physical properties are phenomenologically shown in fig. 5. Further in a PCM storage, due to encapsulation and thus void fraction, the density difference $\rho_s \leftrightarrow \rho_l$ with $\rho_s > \rho_l$, and necessary heat transfer fluid (for example water) for heat transfer in the storage itself, the advantage of a PCM compared to water (around the phase change temperature T_{s-l}) reduces further and further, if the cycled storage temperature difference ΔT is increased. In numbers (table 2), the PCM storage compared to a water storage, (RT15: ρ_s(-15 °C)=0.88 kg*l^{-1}) to liquid (l) (ρ_l(20 °C)=0.77 kg*l^{-1}; Δh =150 kJ*kg^{-1}); (RT38: solid (s) ρ_s(20 °C)=0.88 kg*l^{-1} to liquid (l) ρ_l(40 °C)=0.75 kg*l^{-1}; Δh =170 kJ*kg^{-1}) and vice versa. This lower density than water, (ρ_l(40 °C)=0.992 kg*l^{-1}), c_{p_l}(40 °C)= 4.179 kJ*kg^{-1}*K^{-1}; ρ_l(40 °C)*c_{p_l}(40 °C) = 4146.32 kJ*m^{-3}*K^{-1}) and lower thermal capacity $\rho(T)*c_{p,l}$(RT38, 40 °C)=2 kJ*kg^{-1}*K^{-1}, (lower volumetric energy density) for comparison can explain part of the results. The advantage of bare PCM (no immersed heat exchanger considered), in regard the volumetric energy density, is generally restricted to a temperature difference ΔT of 15 K. As soon as the cycled temperature difference ΔT is increasing, PCMs superiority decreases rapidly and the stored energy equals to the energy of a water storage - see figure 5.

The heat capacity $c_{p,NTES}(T)$ (in $kJ*kg^{-1}*K^{-1}$) of an NTES, with sand and water as storage materials ($c_{p,NTES}(T) = a*c_{p,WTES}(T) + b*c_{p,Sand}(T)$; with a+b = 1), lays between the value of sand and water. A NTES size (volume) for the same heat energy capacity as in a WTES (in the same temperature range) is thus larger and an optimum to cover the building demand is shifted to larger volumes. Table 2 contains information about the thermal capacity of storage materials of the used storages. And as mentioned above in figure 5 a phenomenological explanation is given.

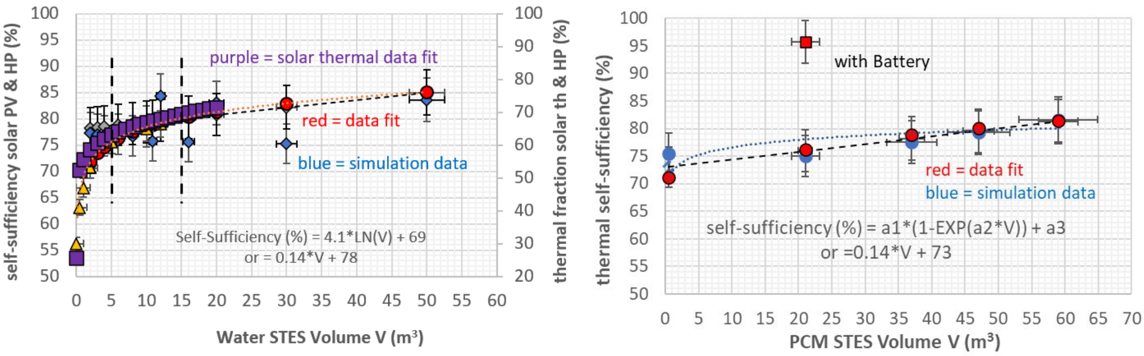

Fig. 3 Thermal self-sufficiency (%) in function of storage size i.e. volume V (m3) of a sensible water STES for a SFH as the reference case (left). In the left graph, solar thermal data with heat pump from (Duffie Beckman 2013) are included. Thermal self-sufficiency (%) in function of STES size for PCM STES (right). A linear fit and a logarithm fit curve to the data show the functional behavior. Due to the implementation of a battery (right, PCM STES) in the system, nearly 100 % thermal self-sufficiency can be reached because the heat pump can be run with electric energy of the battery.

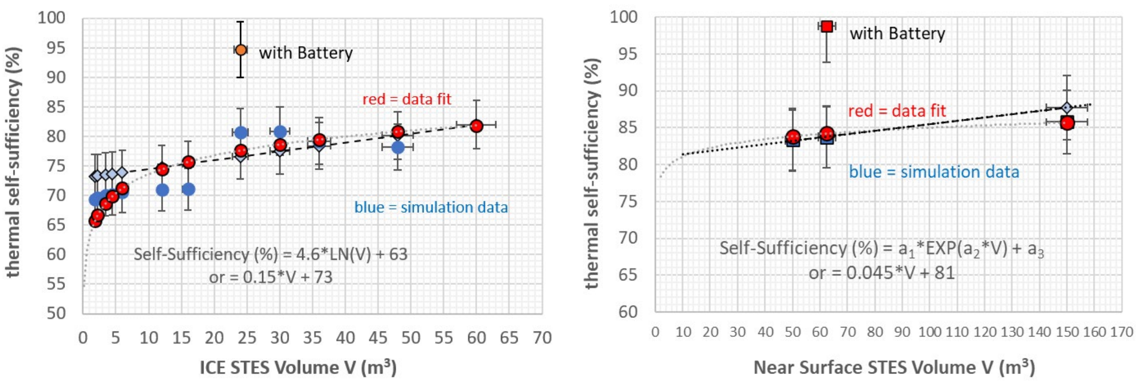

Fig. 4 Thermal self-sufficiency (%) in function of STES size i.e. STES volume V (m^3) or ICE STES (left) and near surface STES (right). For comparison with an ICE STES results for a near surface STES (NTES called eTank [Internet 2026-01-14]) are shown on the right. An eTank consists of humid soil/sand of (general) 10*10*1.5 m^3 size, has an immersed heat exchanger and the eTank position / location is under the building foundation (SFH). And as shown in these graphs, with a battery implemented in the system nearly 100 % thermal self-sufficiency can be reached.

Table 2 List of volumetric heat capacity parameters of storage materials used in the simulations for SFH application.

Storage material (Name)	ρ_l*$c_{p,s}$(T), solid (kJ*m^{-3}*K^{-1})	ρ_l*$c_{p,l}$(T), liquid (kJ*m^{-3}*K^{-1})	Δh_{fus} (kJ*m^{-3})	Remark (-)
WTES (water)*	1832.4 (T < 0 °C)[1]	4176.9 (20 °C)	-	use in the liquid phase ρ(20 °C) = 998.2 kg*m^{-3}
ICE (water)*	1832.4 (T < 0 °C)	4176.9 (20 °C)	305944 (0 °C)	solid and liquid phase; ρ_{ICE}(0 °C) = 916.2 kg*m^{-3}
PCM (organic)#	1540 (solid, T < T_{s-l})	1540 (liquid, T > T_{s-l})	115500 – 192500 (0 – 65 °C)	T_{s-l} @ 15 (°C); heating and cooling use
NTES& (sand & water)	Sand: ~ 2000.0 (20 °C)	Sand: ~ 2000.0 (20 °C)	-	if wet sand; water use in the liquid phase

*VDI-Wärmeatlas, VDI-Gesellschaft Verfahrenstechnik und Chemieingenieurwesen; DOI 10.1007/978-3-642-19981-3. # Rubitherm - https://www.rubitherm.eu/produktkategorie/organische-pcm-rt. & https://ezeit-ingenieure.de/projekt/etank-erdpufferspeicher-langzeitenergiespeicher.

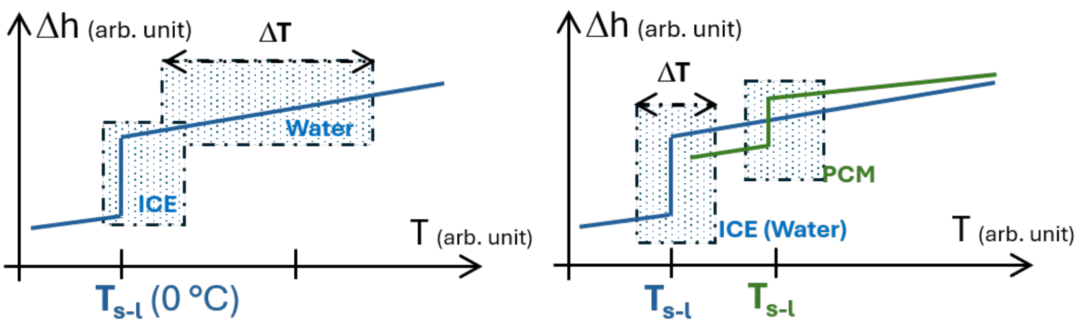

Fig. 5 Phenomenological explanation of the enthalpy changes in function of storage material temperature change (storage temperature cycle from T_{max} to T_{min} with the temperature difference $\Delta T = T_{max}-T_{min}$ and vice versa). (left) ICE and water comparison, (right) ICE and PCM comparison.

The data show that after a certain size of storage (volume V_{STES} in m^3), the thermal self-sufficiency is relatively unsensitive of the size i.e. the volume. And as soon as a battery[2] of 25 kWh (approx. variable value C_{Bat} (kWh) of the battery capacity) electric energy is implemented in the system the thermal self-sufficiency increases up to nearly 100 %. In literature [Stefano Aneli et al. 2023; Michellod et al. 2026; Wang et al. 2025], such results are reported for similar systems implemented in SFH. A further simulation task would be needed to optimize the battery size C_{Bat} in combination with the electric consumers demand profiles. But this is shifted to later work. And due to the lack of a thermo-physical TCM model at this level, the simulation of the thermal (th.) self-sufficiency of a SFH with a TCM STES is post-boned as well. Even if – due to physical reasons - an exponential curve (equation 3) would theoretically fit the data best - all resulting data curves were also fitted with linear and logarithmic equations (equation 1 and 2).

$$th.self\ sufficieny(V) = a_{1\_LN} * LN(V) + a_{2\_LN} \quad \text{(eq. 1)}$$

or

$$th.self\ sufficieny(V) = a_{1\_lin} * V + a_{1\_lin} \quad \text{(eq. 2)}$$

or

$$th.self\ sufficieny(V) = a_{1\_exp} * EXP(a_{2\_exp} * V) + a_{3\_exp} \quad \text{(eq. 3)}$$

---

[1] VDI-Wärmeatlas, VDI-Gesellschaft Verfahrenstechnik und Chemieingenieurwesen; DOI 10.1007/978-3-642-19981-3.

[2] Not optimised battery capacity C_{Bat} (kWh).

Table 2 summarizes the storage size fit parameters for a logarithm fit function, a linear fit function and an exponential fir function of the simulation results shown in figure 3 and, figure 4.

Table 3 storage Volume V fit parameters – logarithm fit function (LN), linear fit function (lin) and exponential fit function (exp).

Storage Type (name)	a_{1_LN} (%)	a_{2_LN} (%)	a_{1_lin} (%)	a_{2_lin} (%)	a_{1_exp} (%)	a_{2_exp} (m^{-3})	a_{3_exp} (%)
WTES (water)	4.1	69	0.14	78	10	-0.05	75
NTES (eTank*)	4.25	66	0.045	81	6	-0.02	80
ICE (water ice)	4.6	63	0.15	73	12	-0.0333	70
PCM (T_{s-1} = 15 °C)	9.1	60.5	0.14	73	15	-0.02	71

*eTank: soil – sand & water, below the building base plate.

Further simulations will be performed by changing the design variable C_{Bat} (kWh) of the battery, i.e. the electric energy capacity C_{Bat} (kWh) of the battery. And in regard of (thermal) self-sufficiency in function of area A_{PV}, volume V_{STES} and capacity C_{Bat} a comparison with solar thermal technology systems will be extended [Duffie Beckman 2013 - and literature therein].

5. Conclusion

Simulation templates for a building energy system with different types and sizes of long-term storages were defined for a single-family house. The performed simulations show results of the thermal self-sufficiency with a size (volume) dependent behavior. And the self-sufficiency in function of volume curves can be fitted – in certain volume ranges - with either a linear, logarithmic or exponential function. The thermal energy storage size (depending on the volumetric energy density) has a strong influence on the thermal self-sufficiency of the single-family house. Independent of the storage type, at volumes below 15 m^3 a strong increase of the thermal self-sufficiency can be observed. And at a volume lager this value, a low, linear dependent increase is visible. But even with a big storage (several tenth of m^3), the thermal self-sufficiency is below 100 %. For contrary, in case the system contains a battery of appropriate storage capacity, the energy system can transfer the building to a “Net Zero” building – both, to thermal and electric self-sufficiency. A characteristic similarity of the (1 from literature) solar fraction and (2 own simulation) thermal self-sufficiency in function of storage volume curves was found. For all types of long-term storage, a storage size optimum seems to be in the volume range of 5 m^3 to 15 m^3. We assume, this value can be optimized by adjusting the size of the small storages (DHW & space heating) in this multiparameter task. Although we did not re-simulate the data from literature - with all the parameters used therein - we conclude a sufficient proof - but not complete (in the mathematical sense) of the similarity. In a next step an optimization of a thermal energy storage size V_{STES} (m^3) in function f of the relations PV field area (m^2) to space heating area A_{SH} (m^2) $V_{STES} = f(A_{PV}/A_{SH})$ could be done. A comparison with a solar thermal collector field, with collector area A_C, system is then obvious. And system design guidelines could then be deduced.

ACKNOWLEGEMENT

We highly acknowledge the Swiss National Science Foundation (SNSF) and OST Eastern Switzerland University of Applied Sciences financing the work about thermal self-sufficiency of buildings and heat losses of large – long-term – thermal energy storages, which was conducted as part in the frame of the SNSF SOTES project CRSII5_202239.

6. References

Matthias Berger, Bejamin Schroeteler, Helene Sperle, Patrizia Püntener, Tom Felder, Jörg Worlitschek, Assessment of residential scale renewable heating solutions with thermal energy storages. Energy 244 (2022) 122618.

https://ezeit-ingenieure.de/projekt/dynamischer-energie-manager-mit-offenem-oszillierendem-speichersystem-demoos/ (2026-01-14).

Mattia Battaglia, Robert Haberl, Evelyn Bamberger, Michel Haller. Increased self-consumption and grid flexibility of PV and heat pump systems with thermal and electrical storage. Energy Procedia 135 (2017) 358-366.

Stefano Aneli et al., Improvement of energy self-sufficiency in residential buildings by using solar-assisted heat pumps and thermal and electrical storage. Sustainable Energy Technologies and Assessments 60 (2023) 103446. https://doi.org/10.1016/j.seta.2023.103446.

Steffen Schedler, Stefanie Meilinger, Tanja Clees. A new bottom-up method for classifying a building portfolio by building type, self-sufficiency rate, and access to local grid infrastructure for storage demand analysis.

Applied Energy 371 (2024) 123502. https://doi.org/10.1016/j.apenergy.2024.123502.

Mart van der Kam, Alejandro Pena-Bello, David Parra. PV for what? A PV self-sufficiency analysis of electric vehicles, heat pumps, and home storage. Energy 334 (2025) 137774. https://doi.org/10.1016/j.energy.2025.137774.

Saeed Rayegan, Ali Katal, Liangzhu (Leon) Wang, Radu Zmeureanu, Ursula Eicker, Mohammad Mortezazadeh, Sepehrdad Tahmasebi. Modeling building energy self-sufficiency of using rooftop photovoltaics on an urban scale. Building & Energy 324 (2024) 114863. https://doi.org/10.1016/j.enbuild.2024.114863.

Julien L. Michellod, Arbogast Nyandwi, Arven Syla, Francesco Sasso, Martin K- Patel, Selin Yilmaz. Self-consumption and self-sufficiency of the Swiss residential stock: Building archetypes for simulation of positive energy districts. Sustainable Cities and Society 129 (2025) 106486. https://doi.org/10.1016/j.scs.2025.106486.

Zheng Wang, Mark Luther, Peter Horan, Jane Matthews, Chunlu Liu. Residential space heating electrification through a PV-driven hot water heat pump. Energy and Buildings, Volume 330, 1 March 2025, 115319.

John A. Duffie and William A. Beckman. Solar Engineering of Thermal Processes. WILEY ISBN 978-0-470-87366-3.

C. Dennis Barley and C. Byron winn. Optimal sizing of solar collectors by the method of relative areas. Solar Energy Vol. 21, pp. 279-289.

J. V. Anderson, j. W. Mitchell and w. A. Beckman. A design method for parallel solar-heat pump system. Solar Energy Vol. 25, pp. 155-163.

Appendix:

1. NOMENCLATURE AND SYMBOLS

Table A1: Symbols for quantities

Quantity	Symbol	Unit
Area	A	m^2
Fit Parameter	a	-
Solar irradiance	G^*	$W\ m^{-2}$
Mass flow rate	$\dot{m}$	$kg\ s^{-1}$
Heat	Q	J
Heat flow rate	$\dot{Q}$	W
Heat of fusion	Δh_{fus}	$kJ\ kg^{-1}$
Temperature	T, t	°C, K
Temperature difference	ΔT	K
Power (el., HP etc.)	P	W, kW
Efficiency	η	-
Time	t	s

Table A2: Subscripts of quantities

Quantity	Symbol
Ambient	*a*
Battery	*Bat*
Buffer Tank (space heating SH)	*Buffer*
Energy demand (el., DHW, SH)	*demand*
Solar Thermal Collector	*C*
Domestic Hot Water	*DHW*
Heat pump	*HP*
Linear	*l*
logarithmic	*ln*
Number (even)	*1, 2, 3, …*
Mean	*m*
Outside atmosphere	*o*
Photovoltaic	*PV*
Room (heating, living)	*room*
Seasonal Thermal Energy Storage	*STES*
Space Heating	*SH*
thermal	*th*

2. FIGURES FROM LITERATURE

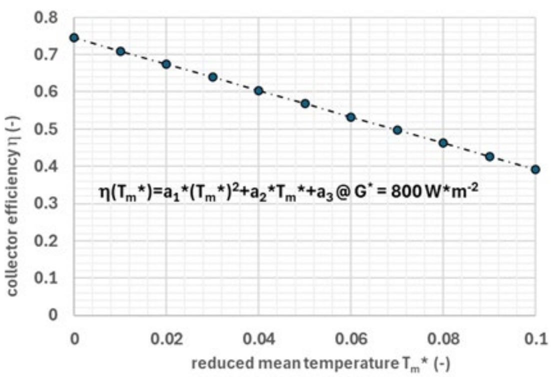

Fig. 6 Example of a solar thermal collector efficiency η curve in function of the reduced mean temperature T_m, https://spftesting.info/data/1.collectors/.*

Figure 5 shows the efficiency η (-) curve in function of T_m^*= ($W\ m^{-2}\ K^{-1}$) of a solar thermal collector. Were t_m (°C) the mean collector temperature, t_a (°C) ambient temperature and G* ($W\ m^{-2}$) global hemispherical solar irradiance T_m^*= ($W\ m^{-2}\ K^{-1}$).

$$T_m^* = \frac{(t_m - t_a)}{G^*}$$

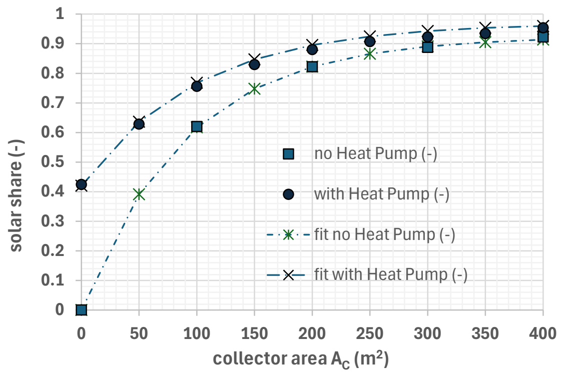

Fig. 7 Solar share in function of collector area A_c of a solar thermal collector system – (I) no Heat Pump and (II) with Heat Pump (hybrid / parallel) - to a building heat energy system (Anderson et al. 1980).

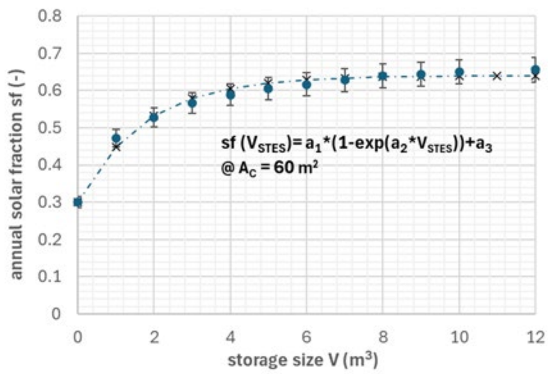

Fig. 8 Annual solar fraction (sf) in function of storage size (V) and a fixed collector area (A_C) of 60 m^2 (Anderson et al. 1980).

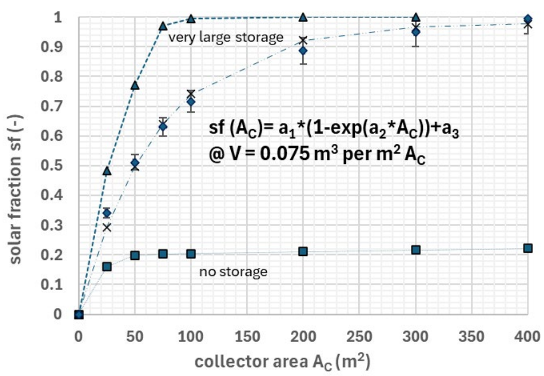

Fig. 9 Annual solar fraction (sf) in function of solar thermal collector area (A_c) and storage size (volume V_{STES} per area A_c) as parameter (Duffie Beckman 2013).